*Manuscript
Click here to view linked References

Enhanced magnetocaloric effect in rapidly solidified $HoNi_2$ melt-spun ribbons

J.L. Sánchez Llamazares,[a,*] P. Ibarra-Gaytán,[a,b] C.F. Sánchez-Valdés,[c] Pablo Álvarez-Alonso,[d] R.Varga[b]

[a]*Instituto Potosino de Investigación Científica y Tecnológica A.C., Camino a la Presa San José 2055, Col. Lomas 4ª, San Luis Potosí, S.L.P. 78216, México.*
[b]*CPM-TI, University Pavol Jozef Safárik, Park Angelinum 9, 04154 Kosice, Slovakia.*
[c]*División Multidisciplinaria, Ciudad Universitaria, Universidad Autónoma de Ciudad Juárez (UACJ), calle José de Jesús Macías Delgado # 18100, Ciudad Juárez 32579, Chihuahua, México.*
[d]*Departamento de Física, Universidad de Oviedo, Calvo Sotelo s/n, 33007 Oviedo, Spain.*

The structural, magnetic and magnetocaloric properties of $HoNi_2$ melt-spun ribbons were investigated by X-ray diffraction, magnetization and specific heat measurements. The as-solidified ribbons samples produced are single phase with the cubic $MgCu_2$-type crystal structure of the Laves phase (C15; space group Fd-3m), and a Curie temperature T_C of 13.9 K. For a magnetic field change $\mu_o\Delta H$ of 5 T (2 T) applied along the ribbon length, the produced ribbon samples show a maximum magnetic entropy change ΔS_M^{peak} of -27.2 (-16.9) J kg^{-1} K^{-1}, a full-width at half-maximum δT_{FWHM} for the $\Delta S_M(T)$ curve of 19 (11) K, and a refrigerant capacity, determined from the area below δT_{FWHM} the $\Delta S_M(T)$ curve, of 388 (145) Jkg^{-1}; the adiabatic temperature change ΔT_{ad} at 2 T is 6.7 K. Whereas crystal structure and intrinsic magnetic properties are in good agreement with the experimental data previously reported in literature for bulk polycrystalline alloys, the magnetocaloric parameters at 2 T are markedly superior owing to the favorable combination of partial texture with the anisotropic behavior of magnetization.

Keywords: $HoNi_2$ Laves phase; melt-spun ribbons; magnetic entropy change; adiabatic temperature change.

*Corresponding author. Email address: jose.sanchez@ipicyt.edu.mx (J.L. Sánchez Llamazares).

I. INTRODUCTION.

In the last twenty years, materials exhibiting a large magnetocaloric effect (MCE) have attracted intense research interest. This has been motivated by the fact that magnetic refrigeration based on MCE is a more energy efficient and environment friendly solid-state cooling technology than the traditional one based on gas compression/expansion [1,2]. Among the magnetocaloric (MC) materials studied for magnetic refrigeration in the cryogenic temperature range, the binary intermetallic Laves phases RNi_2 with the heavy rare-earth elements R= Ho, Tb, Dy, or Er, and related solid solutions, are of potential use for developing active magnetic regenerative refrigerators for gas liquefiers [1-3].

The Laves phase $HoNi_2$ crystallizes into the cubic $MgCu_2$-type crystal structure (C15; space group Fd-3m) [4], being a ferromagnetically ordered compound with a Curie temperature T_C around 14 K whose magnetism comes from Ho^{+3} ions [5-10]. Magnetization measurements performed on a single crystalline sample at 1.4 K demonstrated that at zero magnetic field the spontaneous magnetization lies along the [100] direction [8], and the spontaneous magnetic moment is 7.55 μ_B/Ho^{+3}, whereas the magnetic moment values measured along the [110] (intermediate) and [111] (hard) directions are 5.34 μ_B/Ho^{+3} and 4.33 μ_B/Ho^{+3}, respectively. These magnetization differences lead to a different, or anisotropic, MC response if the magnetic field is applied along such notable crystallographic directions.

The magnetic field-induced entropy and adiabatic temperature changes curves for $HoNi_2$, i.e., $\Delta S_M(T)$ and $\Delta T_{ad}(T)$, have been theoretically calculated by von Ranke *et al.* [11], and Plaza *et al.* [12] whereas experimental studies on bulk polycrystalline alloys produced by arc melting have been carried out by Tomoyiko *et al.* [10], Gomes *et al.* [13], Singh *et al.* [5], and Cwik *et al.* [14]. Normally, the alloys produced by arc melting are subsequently thermally annealed for a long time (from 2 days to a month) at temperatures in the range of 800-1173 K. Present research was undertaken to produce melt-spun polycrystalline ribbons of this binary intermetallic compound in order to investigate their MC properties. The results obtained are compared with those previously reported for bulk polycrystalline samples. This processing technique has been recently applied to fabricate ribbon samples of other Laves phases of the same family, such as $TbNi_2$ and $DyNi_2$ with R = Tb or Dy [15,16], with positive results.

II. EXPERIMENTAL PROCEDURE

An as-cast bulk ingot of nominal stoichiometric composition $HoNi_2$ was produced by argon arc melting from highly pure elements: Ho (99.9 %, Sigma Aldrich) and Ni (99.99 %, Alfa Aesar). The sample was melted three times to assure a good starting homogeneous mixture of the raw elements. Melt-spun ribbons were obtained from this arc-melted ingot in an UHP Ar atmosphere at a linear speed of the rotating copper wheel of 20 ms^{-1}; the process was carried out using the Edmund Bühler model SC melt spinner system.

The room temperature X-ray diffraction (XRD) pattern of finely powdered ribbons was collected with a Rigaku Smartlab high-resolution diffractometer using Cu-K_α radiation (λ = 1.5418 Å). The scan was made in the interval $20^o \leq 2\theta \leq 100^o$ with 0.01^o of 2θ step increment. Scanning electron microscopy (SEM) observations and energy dispersive spectroscopy (EDS) analyses were done in a FEI Helios Nanolab 600 dual beam FIB/SEM scanning electron microscope (SEM).

Magnetic measurements were performed by vibrating sample magnetometry in a 9 Tesla Quantum Design (QD) PPMS® Dynacool® system. The magnetic field $\mu_o H$ was applied along the ribbon axis (i.e., the rolling direction) to minimize the effect of the internal demagnetizing field. Magnetization as a function of temperature $M(T)$ curves were measured under a low (5 mT) and high (5 T) static magnetic fields with a temperature sweeping rate of 1.0 $Kmin^{-1}$. The relaxation method using the heat capacity (HC) option of a 9 Tesla Quantum Design PPMS® Evercool®-I system was used to determine the specific heat c_p as a function of the temperature curves from 2 to 50 K (the increment in T between two successive c_p data points was 0.25 K). Measurements were executed using the vertical HC puck; thus, as for magnetization measurements, the magnetic field was applied along the longitudinal direction of the melt-spun ribbons. Ribbons samples with average masses of 0.00215 and 0.00224 g were used for magnetization and specific heat measurements, respectively (they were weighted 12 times); the uncertainty in mass determination was ± 1.0 x 10^{-5} g.

III. RESULTS AND DISCUSSION

Figures 1(a), (b) and (c) show characteristic SEM micrographs of the cross-section (fractured morphology), wheel surface and free surface microstructure of the synthesized as-quenched (aq) ribbons. Ribbons are polycrystalline with an average thickness of 25-30 μm. At the ribbon surface that makes contact with the Cu wheel during solidification, the much faster cooling rate

forms a thin layer of small disordered grains whose morphology and average grain size is very different from the observed from the end of such layer up to the free ribbon surface. As the cross-sectional micrograph shows, elongated grains grow through that thicker region whose longer axis tends to be aligned perpendicular to the ribbon surface (i.e., along the thermal gradient during solidification). If true that the preferred grain orientation is far from being perfect, is a signature of some crystallographic texture in the synthesized ribbon samples. The fractured cross section of many ribbon samples was observed confirming this regularity. From more than 20 EDS spectra (not shown), collected from the ribbons surface and cross section, it was determined that within the experimental error (typically 0.1 at. %), the elemental chemical composition of the fabricated ribbons is close to the nominal one, i.e., 1:2. Figure 2(a) shows the experimental X-ray powder diffraction pattern and its Rietveld refinement achieved with the FULLPROF suite package.[17] As shown in the figure, all the diffraction Bragg reflections were properly identified and indexed on the basis of the cubic $MgCu_2$-type crystal structure (C15) of Laves phase (space group Fd-3m; PDF card 04-001-1834). No trace of a different phase was observed. As listed in Table 1, the determined lattice parameter, a = 7.1497(3) Å, is reasonably in agreement with the reported in literature for bulk alloys [5,14,18]. Hence, the processing technique employed simplifies the fabrication procedure in the sense that circumvents the long-term high-temperature thermal annealing usually used to produce single-phase alloys prepared by a conventional melting process.

The temperature dependencies of the magnetization $M(T)$ measured under low- and high-static magnetic field values of 5 mT and 5 T are shown in Figure 2(b); while the inset displays the dM/dT vs. T curve at 5 mT in the vicinity of the second-order magnetic phase transition. Ribbon samples exhibit a sharp magnetic phase transition; the T_C, estimated from the $dM/dT(T)$ minimum, was 13.9 K, a value that agrees with the reported in literature for bulk alloys (that varies between 13 and 14 K) [5,6,9,10,11,13,14], whereas the saturation magnetization at 2.0 K and 5 T is 159.0 A m^2 kg^{-1}.

Figures 3(a) shows the set of isothermal $M(\mu_o H)$ curves measured from 2 to 50 K up to 5 T through the magnetic phase transition. The temperature increment between two consecutive curves was 1.0 K. The $\Delta S_M(T)$ curves at 5 and 2 T determined from these data by means of numerical integration of the Maxwell relation are plotted in Figure 4(a) and (b), respectively. Figure 3(b) shows the temperature dependence of the specific heat $c_p(T)$ at 0 and 2 T. From these $c_p(T)$ curves, the thermal dependencies of the total entropy $S_T(T)$ were obtained through the

relation $S_T(T,B) = \int_0^T \left[\frac{c_p(T',B)}{T}\right] dT' + S_o$; they are shown at the inset of Figure 3(b). At zero field, $c_p(T)$ presents the typical λ-type shaped peak located at T_C of a ferromagnet (from the curve the T_C value determined was 13.7 K). The increase in the applied magnetic field results in the expansion and reduction of the height of the $c_p(T)$ peak. The $c_p(T)$ values measured are consistent with those previously reported in literature [5,14,19,20]. Considering isentropic and adiabatic processes the $\Delta S_M(T)$ and $\Delta T_{ad}(T)$ curves were traced; these curves are compare in Figure 4 with those reported in literature for bulk polycrystalline alloys. Table 2 complements the comparison. The table compares the significant magnetocaloric parameters of melt-spun ribbons and bulk polycrystalline alloys. This includes the estimated values for the refrigerant capacity *RC*, that were determined following the three different criteria established in literature [21-23]: (a) by finding the product $|\Delta S_M^{peak}|$ x δT_{FWHM} (*RC*-1), where δT_{FWHM} is the full-width at half-maximum of the $\Delta S_M(T)$ curve, i.e., $\delta T_{FWHM} = T_{hot} - T_{cold}$, and is usually assumed as the working temperature span of the thermodynamic cycle being T_{hot} and T_{cold} the hot and cold ends, respectively; (b) by calculating the value of the integral area under the $\Delta S_M(T)$ curve between T_{hot} and T_{cold} (*RC*-2); and (c) by maximizing the product ΔS_M x δT below the $\Delta S_M(T)$ curve (*RC*-3). Though these criteria have widely used by the MC community, they consider the entire refrigerant at the same temperature, a condition not fulfilled for the refrigerant in any active magnetic regenerator where a *T* gradient exists along the material, and do not take into account that the refrigerant must exhibit a high enough adiabatic temperature change at the hot and cold ends to allow an efficient heat transfer [24]. As shown below, the last condition is accomplished by $HoNi_2$ ribbons as they show a significant adiabatic temperature change. In a recent manuscript, *Brück et al*. proposed a dimensionless figure of merit, called the coefficient of refrigeration performance (CRP), that considers the relationship between the cooling work during a cycle with the positive work done on the refrigerant [25]. The estimated value of CRP at 2 T for the fabricated ribbon is 0.31 (that is higher than the estimated for the same field change value of 0.22 obtained by these authors for the benchmark room-temperature MC material Gd).

Focusing on the MC response obtained for a magnetic field change of 2 T (the highest value of interest from the viewpoint of potential refrigeration application), it must be noticed that the $|\Delta S_M^{peak}|$ value determined from both magnetization and specific heat measurements, as well as the shape of the respective $\Delta S_M(T)$ curves, are greatly in agreement. This means that we have obtained reliable values for the magnetocaloric effect from both kinds of measurements. It is noteworthy that, in comparison with the data reported for bulk polycrystalline alloys [5,10,14],

the as-solidified melt-spun ribbon samples produced show superior $|\Delta S_M^{peak}|$ (16.9 versus 14.3 and 14.6 $Jkg^{-1}K^{-1}$) [14], and ΔT_{ad}^{peak} (6.7 K versus 4.6 and 4.2 K [14]) values. Consequently, this also leads to a larger refrigerant capacity. A similar result was previously observed in the case of $DyNi_2$ as-solidified ribbons [16], and has been mainly attributed to the favorable combination of partial grain orientation, that leads to some degree of crystallographic texture along ribbon length, and the anisotropic behavior of magnetization in this compound.

In order to get a qualitative verification of such an assumption for the present case, ribbon flakes were finely pulverized with an agate mortar to prepare a cylindrical shaped sample (sample mass: 0.00837 g ± 1.0 x 10^{-5} g). To avoid free powder particle orientation upon the application of the magnetic field during magnetization measurements, a tiny amount of GE-7031 varnish was added to the cylindrical VSM powder sample holder (QD part No. P125E); a second sample holder (identical in shape, but male) was used to slightly compress the sample and seal the combination. Ultrasonic cavitation was used to disperse particles prior varnish solidification. For this sample, that will be referred hereafter as "pulverized ribbons", we measure a set of $M(\mu_o H)$ curves up to a maximum applied external magnetic field of 6 T; the curves were properly corrected due the internal demagnetizing field. In Figure 5(a) and its inset, we compare the non-normalized and normalized (to the maximum magnetization value M_S at 5 T) isothermal magnetization curves at 2 K for both ribbons and a sample of pressed pulverized ribbons. It must be noticed that the magnetization curve for the ribbon samples displays a well-faster approach to saturation with respect to that of the pulverized one; in order to visualize better the difference between both curves, the $\mu_o H$ axis in the foreground graph has been limited to 3 T. It is well known, that in alloys with a high crystallization kinetics the high solidification gradient during ribbon fabrication induces grain orientation and consequently partial or nearly total crystallographic texture. In this case, such a partial grain alignment is revealed by SEM images of ribbons cross-section. On the other hand, the faster approach to saturation of magnetization that the isothermal magnetization curve shows that a certain volume faction of the grains in the sample are aligned with their (100) planes close to the rolling direction leading the observed enhancement in the magnetocaloric properties for a lower magnetic field change with respect to the polycrystalline bulk alloys, where the crystalline domains are presumed to be randomly distributed. At last, it must also be considered that when measuring the magnetocaloric properties the results that many authors report correspond to the external applied magnetic field, and the effect of the internal demagnetizing field is simply neglected or not considered. "In order to show better the beneficial effect of the partial grain orientation of melt-spun ribbons on their

magnetocaloric properties, the $\Delta S_M(T)$ curves at 5 and 2 T for both ribbons and pressed pulverized ribbons are compare in figure 5(b); the meaningful magnetocaloric parameters are listed in Table 2. In addition, the inset of the figure shows the $|\Delta S_M^{peak}|$ versus $\mu_o \Delta H$ dependence for both samples. Focusing on the temperature span delimited by the full-width at half-maximum, the curves, melt-spun ribbons systematically show larger ΔS_M values for both magnetic field changes than the obtained for pulverized ribbons. The dependence of $|\Delta S_M^{peak}|$ on $\mu_o \Delta H$ also shows a similar trend."

IV. CONCLUSIONS.

In conclusion, in this work we report the fabrication of single-phase melt-spun ribbons of the binary Laves phase $HoNi_2$ with the Mg_2Cu-type crystal structure and the characterization of their magnetocaloric properties from magnetization and specific heat measurements. The comparison of our experimental results for a magnetic field change of 2 T with those reported in literature for bulk polycrystalline alloys proves that the as-solidified ribbon samples produced exhibit enhanced magnetocaloric properties along the ribbon longitudinal length, that derives from a favorable combination of the partial grain orientation (texture effect) induced by the high thermal gradient during solidification and the anisotropic behavior of magnetization of this compound.

ACKNOWLEDGEMENTS

The authors acknowledge the scientific support received from Laboratorio Nacional de Nanociencias y Nanotecnología (LINAN, IPICyT) where the study of structural, magnetic and magneto-thermal properties of samples was conducted. Our gratefulness to M.Sc. B.A. Rivera-Escoto, M.Sc. A.I. Peña Maldonado and Dr. G.J. Labrada-Delgado for their technical support. P.J. Ibarra-Gaytán thanks to CONACYT for supporting his postdoctoral position at UPJS, Kosice, Slovakia. C.F. Sánchez-Valdés is grateful to DMCU-UACJ for supporting his research stays at IPICyT (program PFCE and academic mobility grant); also, for the financial support received from PRODEP-SEP, Mexico (Grant No. UACJ- PTC-383). P. Alvarez-Alonso acknowledges the support received from Asturias Government (FC-15-GRUPIN14-037 245), and MINECO (MAT2014-56116-C4-3-4-R), Spain.

REFERENCES

[1] K.A. Gschneidner Jr., K. Pecharsky, and A.O. Tsokol, Rep. Prog. Phys. **68** (2005) 1479.

[2] V. Franco, J.S. Blázquez, J.J. Ipus, J.Y. Law, L.M. Moreno-Ramírez, and A. Conde, Prog. Mater. Sci, **93** (2018) 112.

[3] S. Jeong, Cryogenics **62** (2014) 193.

[4] Zhou Huaiying and Ou Xiangli, J. Alloys Compd. **177** (1991) 101.

[5] Niraj K. Singh, S. Agarwal, K.G. Suresh, R. Nirmala, A.K. Nigam, S.K. Malik, Phys. Rev. B **72** (2005) 014452.

[6] E.A. Goremychkin, I. Natkaniec, E. Muhle, O.D. Chistyakov, J. Magn. Magn. Mater. **81** (1989) 63.

[7] A.M. Gomes, I.S. Oliveira, and A.P. Guimaraes, A.L. Lima, P. J. von Ranke, J. Appl. Phys. **93** (2003) 6939.

[8] D. Gignoux, F. Givord, and R. Lemaire, Phys. Rev. B **12** (1975) 3878.

[9] A. Castets, D. Gignoux, B. Hennion, R.M. Nicklow J. App. Phys. **53** (1982) 1979.

[10] A. Tomokiyo, H. Yayama, H. Wakabayashi, T. Kuzuhara, T. Hashimoto, M. Sahashi, K. Inomata, Adv. Cryo. Eng., **32** (1986) 295.

[11] P.J. von Ranke, E.P. Nóbrega, I.G. de Oliveira, A.M. Gomes, R.S. Sarthour, Phys. Rev. B **63** (2001) 184406.

[12] E.J.R. Plaza, V.S.R. de Sousa, M.S. Reis, and P.J. von Ranke, J. Alloys Compd. **505** (2010) 357.

[13] A.M. Gomes, I.S. Oliveira, and A.P. Guimaraes, A.L. Lima, P.J. von Ranke, J. Appl. Phys. **93** (2003) 6939.

[14] J. Cwik, Y. Koshkidko, K. Nenkov, E.A. Tereshina, K. Rogacki, J. Alloys Comp. **735** (2017) 1088.

[15] J.L. Sánchez Llamazares, C.F. Sánchez-Valdés, P.J. Ibarra-Gaytán, P. Álvarez-Alonso, P. Gorria, J. A. Blanco, J. Appl. Phys. **113** (2013) 17A912.

[16] P. Ibarra-Gaytán, C.F. Sánchez-Valdés, J.L. Sánchez Llamazares, P. Álvarez-Alonso, P. Gorria, J.A. Blanco, Appl. Phys. Lett. **103** (2013) 152401.

[17] J. Rodrıguez Carvajal, Physica B **192** (1993) 55.

[18] K. Nassau, L.V. Cherry, W.E. Wallace, Phys. Chem. Solids **16** (1960) 123.

[19] J. Cwik, T. Palewski, K. Nenkov, N.V. Tristan, J. Warchulska, G.S. Burkhanov, O.D. Chistyakov, J. Alloys Compd. **373** (2004) 78.

[20] J. Cwik, T. Palewski, K. Nenkov, G.S. Burkhanov, J. Alloys Compd. **399** (2005) 7.

[21] A.M. Tishin, Y.I. Spichkin, The Magnetocaloric Effect and its Applications, IOP, Bristol, 2003.

[22] M.E. Wood, W.H. Potter, Cryogenics **25** (1985) 667.

[23] K.A. Gschneidner Jr., V.K. Pecharsky, A.O. Pecharsky, C.B. Zimm, Mater. Sci. Forum **315-317** (1999) 69.

[24] A. Smith, C.R.H. Bahl, R. Bjørk, K. Engelbrecht, K.K. Nielsen, N. Pryds, Adv. Energy Mater. 2 (2012) 1288.

[25] Ekkes Brück, Hargen Yibole, Lian Zhang, Phil. Trans. R. Soc. A **374** (2016) 20150303.

FIGURE CAPTIONS

Fig. 1. SEM micrographs showing the typical microstructure of ribbons: (a) fractured cross-section; (b) wheel surface, and; (a) free surface.

Fig. 2. (a) Experimental and Rietveld refinement of the room temperature X-ray power diffraction pattern. (b) $M(T)$ curves measured at 5 mT (full red symbols; FC), and 5 T (full black symbols; FH). Inset: dM/d$T(T)$ curve at 5 mT; T_C= 13.9 K.

Fig. 3. (a) Isothermal magnetization curves measured up to a maximum magnetic field of 5 T between 2 and 50 K. (b). Specific heat as a function of temperature measured at 0 and under an applied magnetic field of 2 T. Inset: corresponding $S_T(T)$ curves.

Fig. 4. $\Delta S_M(T)$ curves at $\mu_o\Delta H$ = 2 (a) and 5 T (b) for the fabricated as-solidified melt-spun ribbons compared with the experimental data reported in literature for bulk alloys. (d) $\Delta T_{ad}(T)$ curve at 2 T for the as-solidified melt-spun ribbons compared with the experimental data reported in literature for bulk alloys.

Fig. 5. (a) Isothermal magnetization curve measured at 2 K up to a maximum magnetic field of 5 T for as-solidified and pressed pulverized ribbons. Inset: the same curves normalized to the magnetization value at 5 T (M/M_S^{5T}). (b) Comparison of the $\Delta S_M(T)$ curves at $\mu_o\Delta H$ = 2 and 5 T for as-solidified and pulverized (pulv.) ribbon samples. Inset: $|\Delta S_M^{peak}|$ as a function of $\mu_o\Delta H$ for both samples.

TABLE CAPTIONS

Table 1. Structural and magnetic data for as-solidified $HoNi_2$ melt-spun ribbons compared with the data reported in literature for bulk alloys.

Table 2. ΔT_{ad}^{max}, $|\Delta S_M^{peak}|$, refrigerant capacities RC-1, RC-2, and RC-3, and δT_{FWHM} of the $\Delta S_M(T)$ curve (for $\mu_o\Delta H$ = 2 T and 5 T) for as-quenched and pressed pulverized $HoNi_2$ melt-spun

ribbons. The results are compared with both pressed pulverized ribbons and the data reported in literature for bulk polycrystalline alloys.

Table 1. Structural and magnetic data for as-solidified $HoNi_2$ melt-spun ribbons compared with the data reported in literature for bulk alloys.

Alloy type	a (Å)	T_C (K)	M_S^{5T} (2 K) (A m^2 kg^{-1})
$HoNi_2$ ribbons	7.1497(3) [a]	13.9 [a]	159 [a]
$HoNi_2$ bulk alloys	7.167(1),[5] 7.142,[14] 7.13[18]	14[5], 15[6], 13.1[7], 13.4[8], 13[9], 13[10], 13.5[14]	-

[a] *This work*

Table 2. ΔT_{ad}^{max}, $|\Delta S_M^{peak}|$, refrigerant capacities *RC*-1, *RC*-2, and *RC*-3, and δT_{FWHM} of the $\Delta S_M(T)$ curve (for $\mu_0\Delta H$ = 2 T and 5 T) for as-quenched $HoNi_2$ melt-spun ribbons. The results are compared with the data reported in literature for bulk polycrystalline alloys and the one obtained for the pulverized ribbons.

Method	**Magnetization measurements**								**Specific heat**						**Direct ΔT_{ad}**[14]	
Alloy type	**aq-ribbons**		**pulv. ribbons**		**bulk**[10]		**bulk**[14]		**aq-ribbons**		**bulk**[5]		**bulk**[14]		**measure**	
$\mu_0\Delta H$ (T)	**2**	**5**	**2**	**5**	**2**	**5**	**2**	**5**	**2**	**5**	**2**	**5**[e]	**2**[c]	**5**	**2**	**5**
ΔT_{ad}^{max} (K)	-	-	-	-	-	-	-	-	6.7	-	-	10 [a]	4.6 [a]	-	4.2 [a]	8.7 [a]
$\lvert\Delta S_M^{peak}\rvert$ (Jkg^{-1}K^{-1})	16.9	27.2	14.8	24.8	-	22.3 [a]	14.3 [a]	26.1 [a]	18.4	-	-	24.8 [a]	14.6 [a]	-	-	-
***RC*-1 (Jkg^{-1})**	194	522	169	465	-	400 [a]	145 [a]	468 [a]	216	-	-	389 [a]	173 [a]	-	-	-
***RC*-2 (Jkg^{-1})**	145	388	127	349	-	317 [a]	109 [a]	355 [a]	161	-	-	302 [a]	130 [a]	-	-	-
δT_{FWHM} (K)	11	19	12	18	-	18 [a]	10 [a]	18 [a]	11	-	-	16 [a]	11.7 [a]	-	-	-
T_{hot} (K)	20	27	21	27	-	26 [a]	18 [a]	25 [a]	21	-	-	25 [a]	19.5	-	-	-
T_{cold} (K)	9	8	9	9	-	8 [a]	7.9 [a]	7 [a]	10	-	-	9 [a]	7.7 [a]	-	-	-
RC-3 (Jkg^{-1})	101	267	86	240	-	-	-	-	111	-	-	-	-	-	-	-
$\delta T^{RC\text{-}3}$ (K)	14	23	13	24	-	-	-	-	14	-	-	-	-	-	-	-
$T_{hot}^{RC\text{-}3}$ (K) [b]	22	30	22	31	-	-	-	-	23	-	-	-	-	-	-	-
$T_{cold}^{RC\text{-}3}$ (K) [b]	8	7	9	7	-	-	-	-	9	-	-	-	-	-	-	-

[a] *Estimated value from the reported curves.* [b] *related to RC-3.*

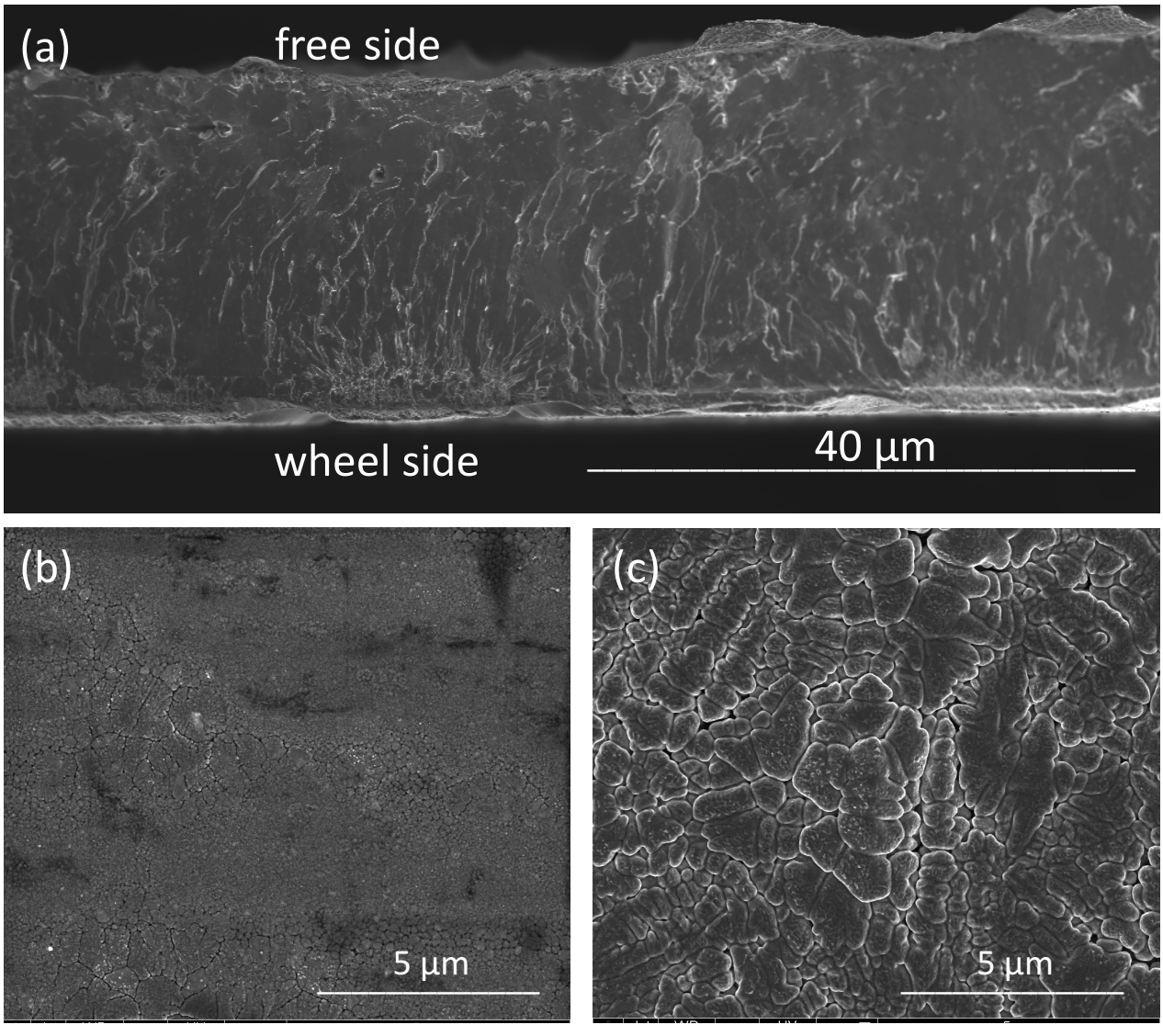

Fig. 1.

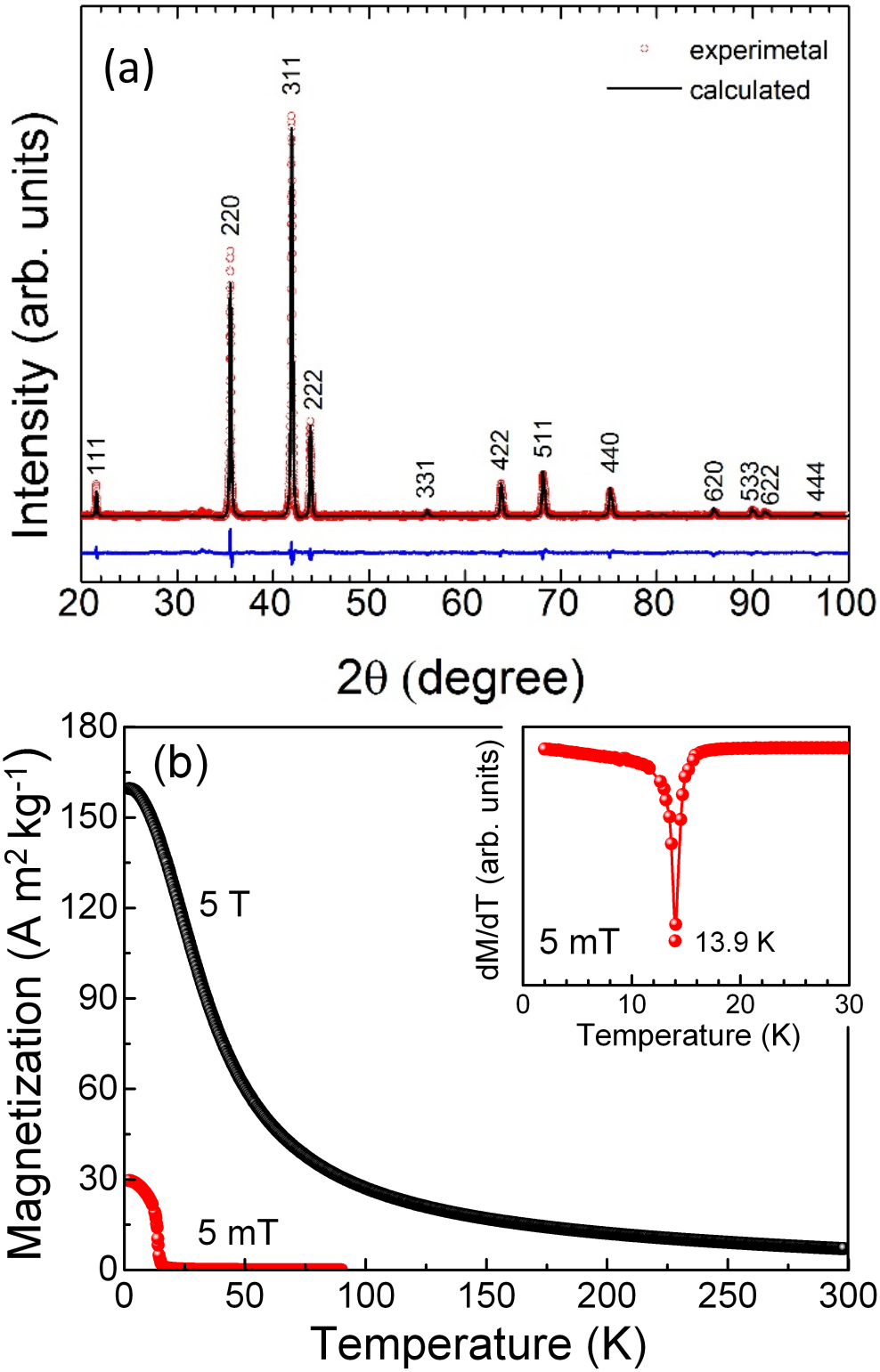
(a)
experimetal
calculated
Intensity (arb. units)
111
220
311
222
331
422
511
440
620
533
622
444
20
30
40
50
60
70
80
90
100
2θ (degree)
(b)
5 T
5 mT
Magnetization (A m2 kg-1)
0
30
60
90
120
150
180
0
50
100
150
200
250
300
Temperature (K)
dM/dT (arb. units)
5 mT
13.9 K
0
10
20
30
Temperature (K)

Fig. 2.

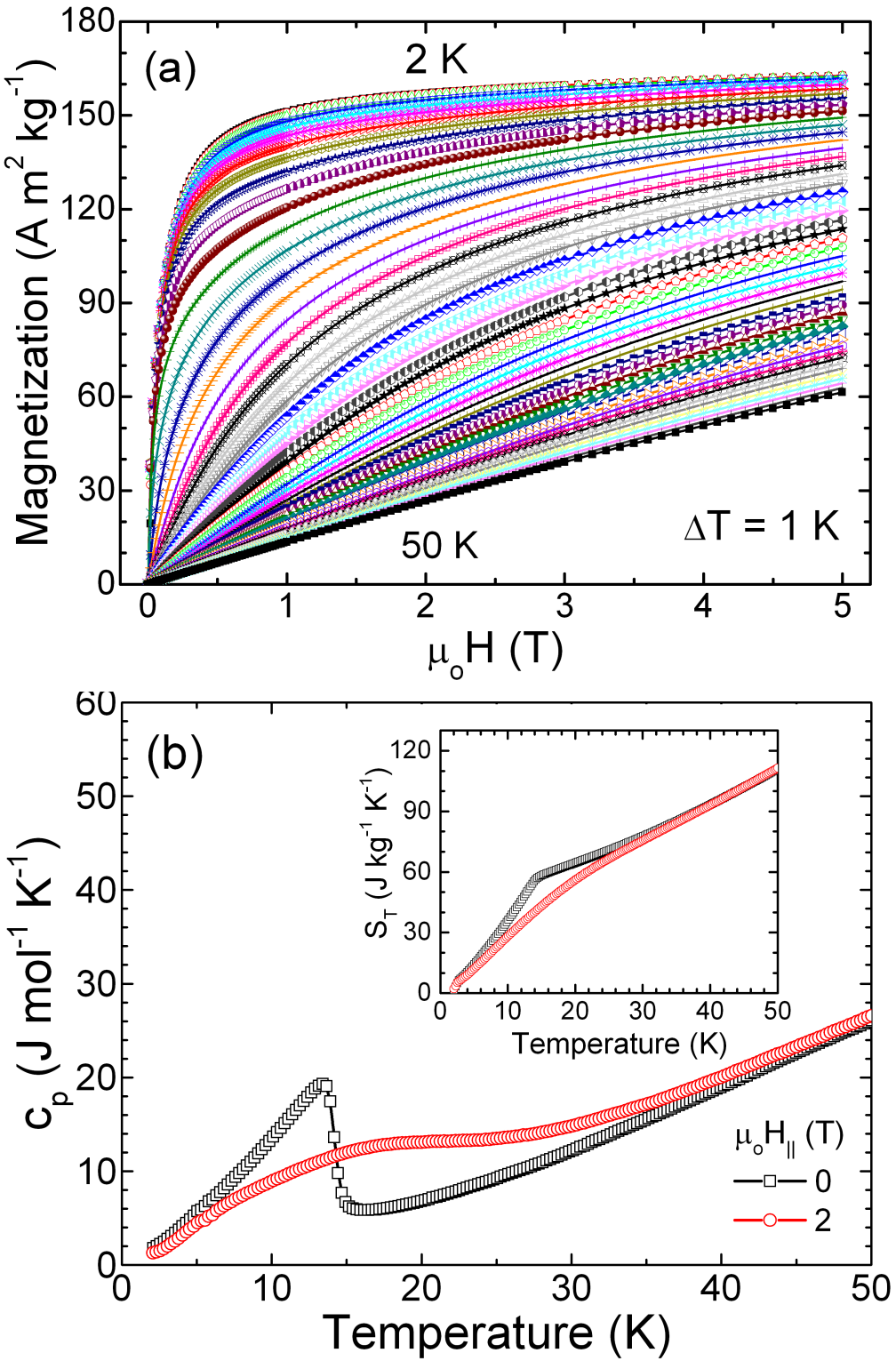
(a)
2 K
50 K
ΔT = 1 K
Magnetization (A m^2 kg^{-1})
μ_oH (T)
(b)
c_p (J mol^{-1} K^{-1})
Temperature (K)
S_T (J kg^{-1} K^{-1})
Temperature (K)
$\mu_o H_{||}$ (T)
0
2

Fig. 3.

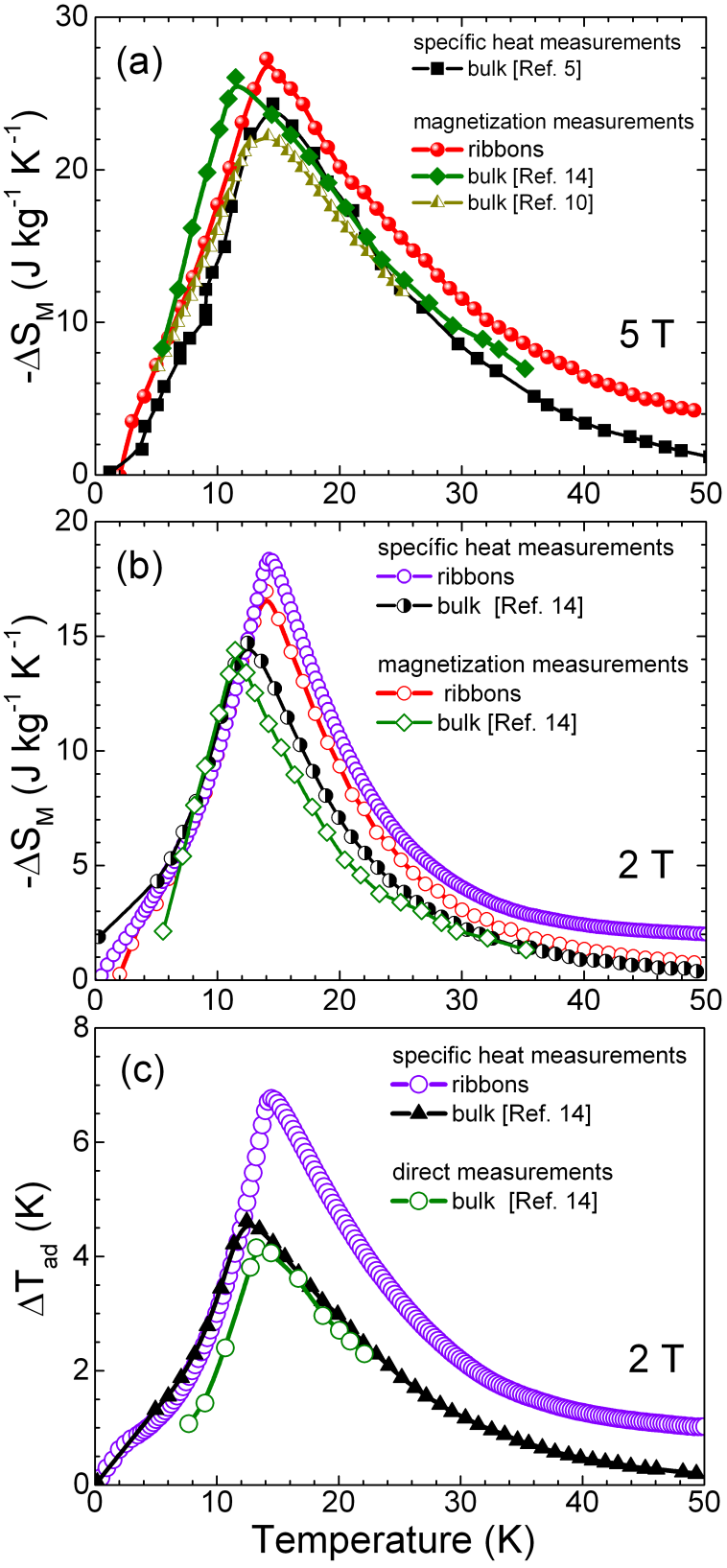
(a)
specific heat measurements
bulk [Ref. 5]
magnetization measurements
ribbons
bulk [Ref. 14]
bulk [Ref. 10]
5 T
-ΔS_M (J kg^-1 K^-1)
(b)
specific heat measurements
ribbons
bulk [Ref. 14]
magnetization measurements
ribbons
bulk [Ref. 14]
2 T
-ΔS_M (J kg^-1 K^-1)
(c)
specific heat measurements
ribbons
bulk [Ref. 14]
direct measurements
bulk [Ref. 14]
2 T
ΔT_ad (K)
Temperature (K)

Fig. 4.

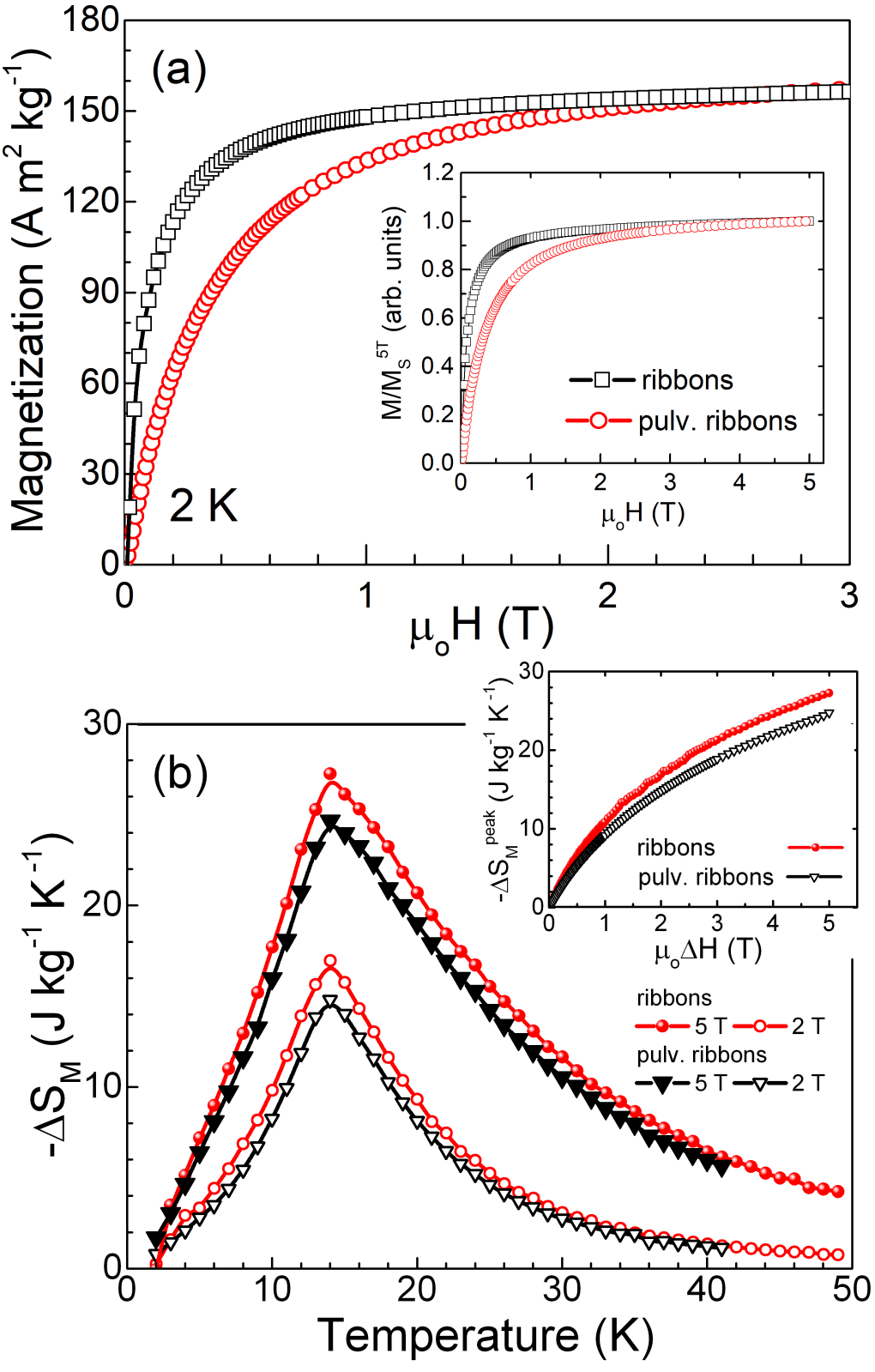
(a)
Magnetization (A m^2 kg^{-1})
2 K
μ_oH (T)
M/M$_S^{5T}$ (arb. units)
ribbons
pulv. ribbons
μ_oH (T)
(b)
-ΔS$_M$ (J kg^{-1} K^{-1})
-ΔS$_M^{peak}$ (J kg^{-1} K^{-1})
ribbons
pulv. ribbons
$\mu_o\Delta$H (T)
ribbons
5 T
2 T
pulv. ribbons
5 T
2 T
Temperature (K)

Fig. 5.

Highlights

- Single-phase ribbon flakes of $HoNi_2$ were fabricated by melt spinning technique.
- Structural, magnetic and magnetocaloric properties of $HoNi_2$ melt-spun ribbons are reported.
- MCE of $HoNi_2$ melt-spun ribbons was studied by magnetization and heat capacity measurements.
- At 2 T, ribbons show larger $|\Delta S_M^{peak}|$ and ΔT_{ad}^{max} values with respect to bulk alloys.